

Towards Guest–Zeolite Interactions: An NMR Spectroscopic Approach

Ding Ma,^{*,[a, d]} Xiuwen Han,^[a] Danhong Zhou,^[a] Zhimin Yan,^[a] Riqiang Fu,^[b] Yide Xu,^[a] Xinhe Bao,^{*,[a]} Hongbing Hu,^[c] and Steve C. F. Au-Yeung^{*,[c]}

Abstract: Guest(metal)–zeolite interactions in a two component heterogeneous catalyst have been investigated by high-field and high-speed ^{27}Al MAS NMR, and two-dimensional ^{27}Al MQ MAS NMR experiments as well as ab initio DFT methods. It was established that strong interactions between guest and zeolite occur in a metal/zeolite

system, with the metal anchored to the tetrahedral aluminum framework site through two oxygen bridges. It disturbs the tetrahedral environment of associ-

ated aluminum framework, changing AlO_4 geometry from near T_d to C_{2v} ; this enables us to resolve this species from the undisturbed aluminum framework species in high-field ^{27}Al MAS NMR and two-dimensional ^{27}Al MQ MAS NMR experiments.

Keywords: host–guest systems • MCM-22 • molybdenum • NMR spectroscopy • zeolites

Introduction

Zeolites are microporous crystalline materials that possess the unique property in functioning as shape-selective catalysts in many reactions.^[1] While metals are among the most important catalysts used since the 19th century,^[2] hosting metal or metal oxide in zeolite results in a so-called bifunctional catalyst^[3] with superior catalytic performances over conventional oxide-supported catalysts.^[4] Examples range from Mo/Y or W/Y for hydro-treatment reactions,^[4a] Ga or Zn/zeolite in light paraffin conversion,^[3b, 4b] Cu/ZSM-5 for NO_x decomposition,^[4c] Ni/SAPO-34 for ethene dimerization,^[4d] Pd/ZSM-5, Fe/ZSM-5 or Co/HZSM-5 for NO reduction by hydrocarbons,^[4e] Pt/

MCM-22 for dehydroisomerization,^[4f] to the recently reported Mo/HZSM-5 or Mo/HMCM-22 for methane aromatization.^[4g] For these metal/zeolite catalysts, initial adsorption/transformation of reactants is believed to take place at the guest center, whereas the zeolite provides channels and acidic sites for sequential reactions. Such combined effects form a synergism that renders the smooth running of catalytic reactions.^[5] Experimental findings have suggested that the metal may replace Brønsted protons, thereby anchoring onto the aluminum framework through the oxygen bridge, so that the active metal center of these bifunctional catalysts is formed.^[4c, 6] Evidence supporting this model were based on a shrinkage of the number of bridging OH groups (Si-OH-Al) in the IR spectrum,^[4e, 7a] or a decrease of the Brønsted peak in ammonia temperature-programmed desorption (TPD- NH_3).^[4e] However, blockage of a channel opening in the zeolite or dehydration of closed Brønsted sites within the zeolite channel catalyzed by adjacent metal species^[7c] equally account for these observations. The splitting peaks observed in the ESR spectra of the metal-loaded zeolite^[7b] (influenced by adjacent $^{27}\text{Al}(\text{I}=5/2)$) is also suggested to serve as a supportive evidence for this model, but is limited to ESR visible metals. Thus, the important issue of whether or not metal is attached to a zeolite framework remains inconclusive. We present here NMR evidence that shows that a strong guest–zeolite interaction is formed.

Result and Discussion

Figure 1 shows the one-dimensional ^{27}Al MAS NMR spectra of MCM-22 and Mo/HMCM-22. HMCM-22 was synthesized following the method of Rubin and Chu^[8] and molybdenum

[a] Dr. D. Ma, Prof. X. Bao, Prof. X. Han, Dr. D. Zhou, Z. Yan, Prof. Y. Xu
State Key Laboratory of Catalysis
Dalian Institute of Chemical Physics
Chinese Academy of Sciences
Dalian 116023 (China)
Fax: (+86) 411-4694447
E-mail: ding.ma@chemistry.oxford.ac.uk, xhbao@dicp.ac.cn

[b] Dr. R. Fu
Center for Interdisciplinary Magnetic Resonance
National High Magnetic Field Laboratory
1800 E. Paul Dirac Drive, Tallahassee, FL 32310 (USA)

[c] Prof. S. C. F. Au-Yeung, H. Hu
Department of Chemistry
The Chinese University of Hong Kong
Hong Kong (China)

[d] Dr. D. Ma
Present address:
Inorganic Chemistry Laboratory, Oxford University
South Parks Road, Oxford, OX1 3QR (UK)

Supporting information for this article is available on the WWW under <http://www.chemieurj.org> or from the author.

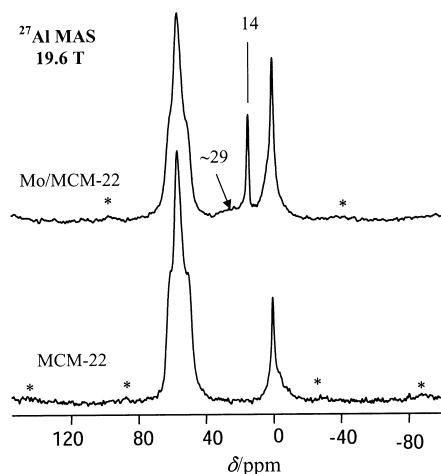


Figure 1. ^{27}Al MAS NMR spectra of MCM-22 and Mo/MCM-22 recorded at 19.6 T. For the conditions of the measurements see the Experimental Section. After the introduction of molybdenum, beside the existence sharp peak at $\delta = 14$ ppm from hydrated aluminum molybdate, a broad peak at around $\delta = 30$ ppm appears.

was introduced into the zeolite by impregnation. The spectrum of MCM-22 shows three peaks at around $\delta = 55$ ppm from tetrahedral framework aluminum in different crystallographically nonequivalent T positions and another peak at $\delta = 0$ ppm from octahedral aluminum.^[9] Loading of molybdenum leads to the appearance of a new peak at $\delta = 14$ ppm. The existence of this kind of peak has been observed on various molybdenum–alumina catalysts, and different formulas have been suggested by different authors.^[10] Considering that a peak at $\delta = -14$ ppm (from $\text{Al}_2(\text{MoO}_4)_3$) is observed in ^{27}Al MAS NMR for the dehydrated Mo/MCM-22 catalyst, which shifts to $\delta = 14$ ppm peak upon hydration (Figure 1 only shows the spectra of full hydrated system), it is reasonable to attribute the signal at $\delta = 14$ ppm to a hydrated species of aluminum molybdate ($\text{Al}_2(\text{MoO}_4)_3$). A tentative formula of $[\{\text{Al}(\text{OH})_n(\text{H}_2\text{O})_{6-n}\}_n](\text{MoO}_4)_3$, has been suggested by Edwards et al. for this full hydrated aluminum molybdate.^[10a,e] The formation of this species is similar to the ligand-promoted alumina dissolution from the alumina surface in Mo/ Al_2O_3 , which is actually a nonframework species.^[10b] At the same time, it is worthwhile to note that the broad peak at around $\delta = 30$ ppm appears at the expense of the main peak at $\delta = 55$ ppm (the intensity of this peak is around 60 % of that of the MCM-22 sample). The origin of the peak at $\delta = 30$ ppm can be attributed to the five-coordinate nonframework aluminum,^[11] the distorted four-coordinate aluminum, or to the overlap of these two species which has recently been established by Grobet et al.,^[12f] Kentgens et al.,^[13] and Fyfe et al.^[12e] Although we cannot make a clear assignment of the species from the one-dimensional MAS NMR spectra, we can conclude at present stage that this signal is inevitably related to the molybdenum because no such species is found in the spectrum of parent MCM-22, when the sample is treated in an identical manner. The formation of this species and the nonframework $[\{\text{Al}(\text{OH})_n(\text{H}_2\text{O})_{6-n}\}_n](\text{MoO}_4)_3$ species indicate the existence of a strong interaction between molybdenum and zeolite framework.

To provide direct evidence and to give an unambiguous assignment to the peak at $\delta = 30$ ppm, we carried out two-dimensional ^{27}Al MQ MAS NMR experiments, in which the second-order quadrupolar line broadening is removed. Therefore species with similar isotropic chemical shifts but different quadrupolar coupling constants can be identified.^[12] By refocusing the second-order quadrupolar anisotropy, through correlation of the evolution of the MQ coherences ($\pm p/2, mp/2$) during t_1 with the single-quantum coherence ($-1/2, +1/2$) of the observable central transition during t_2 ,^[12] a high-resolution spectra in the second dimension is achieved. As demonstrated in Figure 2, the peaks that overlapped at $\delta = 55$

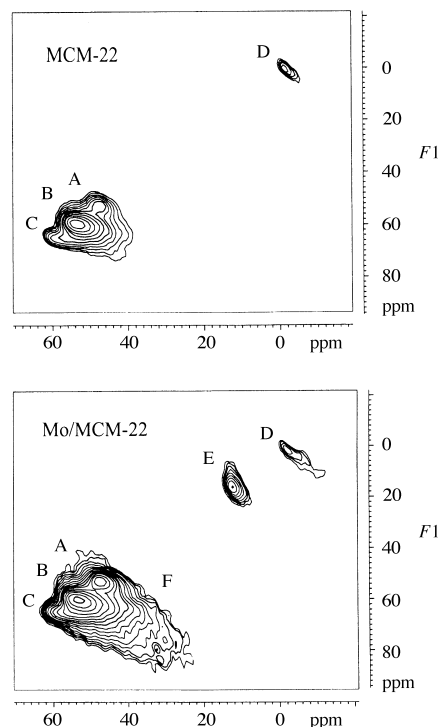


Figure 2. Two-dimensional ^{27}Al MQ MAS NMR spectra of MCM-22 and Mo/MCM-22. The parent zeolite has three tetrahedral framework aluminum species (A, B, and C) and an octahedral Al species (D). With Mo loading, a fifth species E (nonframework) appeared at $\delta \approx 14$ ppm, whereas the presence of F indicates a strong interaction between guest and zeolite.

ppm in Figure 1 are now clearly resolved in the two-dimensional spectra for MCM-22. Three distinct aluminum framework species designated A, B, and C are presented in the tetrahedral region, while the fourth species at $\delta = 0$ ppm (D) is in an octahedral environment. The peak at $\delta = 14$ ppm, which has been attributed to $[\{\text{Al}(\text{OH})_n(\text{H}_2\text{O})_{6-n}\}_n](\text{MoO}_4)_3$, shows a isotropic chemical shift of 14.3 and the second-order quadrupolar effect (SOQE) of 1.5 MHz. The isotropic chemical shifts and the SOQE of these species are summarized in Table 1.

Table 1. Summary of two-dimensional ^{27}Al MQ MAS NMR results.

	A	B	C	D	E	F
δ_{iso} [ppm]	50.6	57.5	62.3	0.1	14.3	54.6
SOQE [MHz]	1.8	2.1	1.9	1.6	1.5	6.2

With the impregnation of molybdenum, additional species F ($\delta_{\text{iso}} = 54.6$ ppm, SOQE = 6.2 MHz, which is difficult to determine due to the very low intensity of this species) is observed in the ^{27}Al MQMAS spectrum of the Mo/MCM-22, as shown in Figure 2. Clearly, this species F appears in the resonance region of the tetrahedral aluminum framework rather than that of the nonframework five-coordinate aluminum. This observation implies that the new peak in MAS NMR experiment after the loading of molybdenum results from a tetrahedral aluminum species. However, the larger SOQE value suggests that species F belongs to a distorted tetrahedral framework species similar to that observed recently in calcinated or hydrothermal-treated zeolite.^[12e,f]

In the present case, the appearance of species F cannot be attributed to the heat-induced distorted tetrahedral Al because the catalyst was calcinated in air at 773 K after impregnation. At this temperature, heat-induced distortion of tetrahedral aluminum (without the help from the molybdenum) is not likely to occur. When MCM-22 was subjected to the identical treatment, the F species was not observed, an indication that the formation of the new tetrahedral coordinated aluminum framework takes place only in the presence of molybdenum.^[14] Other possible formation of such a species is the ex-lattice-aluminum-induced distortion of the tetrahedral aluminum framework, as suggested recently by van Bokhoven et al.^[13] However, such a species (F) is not observed in the spectrum of its parent MCM-22 (which already has ex-lattice aluminum). Thus, it can be concluded that the origin of the species F is related to the impregnation of molybdenum. The large SOQE suggests that the ^{27}Al quadrupole moment of F interacts with an electric field gradient (EFG) larger than that observed in A, B, or C. The correlation of the EFG with the asymmetry of tetrahedral AlO_4 has been reported for many aluminum-containing materials.^[15] Since the four oxygen atoms surrounding Al are predominantly responsible for any electric field present at the Al site in zeolite,^[15b,c] any asymmetry in their distribution would result in lowering the site symmetry. It is well established that the compensation of the Brønsted proton to the zeolite framework results in an highly asymmetric tetrahedral AlO_4 group, that is, the proton-attached Al–O bond is much longer than the other non-proton-attached Al–O bonds and accompanies a change in the bond angles Al–O–Al.^[4e, 17] Such asymmetry leads to a large EFG around the AlO_4 entity. From static ^{27}Al spin-echo NMR experiments or recently developed DFS MQ MAS NMR measurements,^[12g] it was determined that the SOQE value of the protonated tetrahedral framework aluminum zeolite is about 11–16 MHz.^[16a] With adsorption of water, water ion pairs or something similar are formed at these Brønsted centers; this results in a change of Al–O bonds length as well as Al–O–Al bond angles of the concerned AlO_4 tetrahedra.^[16b] Ab initio calculations indicate that the geometry of AlO_4 in dehydrated zeolite recovers from a heavily distorted tetrahedral coordination (with one of its Al–O bond much longer than the rest) to the nearly perfect tetrahedral coordination upon loading the water molecule. As the result, the size of the quadrupole coupling constant of aluminum decreased dramatically (to about 2 MHz, see Table 2). The present samples were fully hydrated in a desiccator filled with

Table 2. Calculated and experimental SOQE values.^[a]

	Z^-	H-Z dehy	H-Z hy	MoZ
calcd SOQE [MHz]	3.6	18	5.4	11.3
exptl SOQE [MHz]	–	11–16 ^[b]	1–3 ^[b]	6–7

[a] Z^- is an AlO_4 entity without the Brønsted proton; H-Z dehy/H-Z hy are the dehydrated and fully hydrated forms, respectively, of the zeolite; MoZ is the tetrahedral aluminum site connected to Mo through an oxygen bridge. [b] Reported in ref. [16].

aqueous NH_4NO_3 , so that the observed signal F cannot be attributed to distorted tetrahedral aluminum induced by dehydration. Meanwhile, the SOQE of this signal (6–7 MHz) is smaller as compared with the dehydrated Brønsted aluminum (11–16 MHz). Through the method introduced by van Santen et al.,^[17] we calculated the local structure and the SOQE value of an AlO_4 entity with and without metal by ab initio DFT methods. We demonstrated that deviation of the AlO_4 coordination from tetrahedral symmetry results when metal is connected to the framework of zeolite (Figure 3).^[4c, 6] Consequently, with a lower site-symmetry at Al, the SOQE becomes larger due to the interaction between the EFG and the quadrupole moment of the ^{27}Al .^[12d, 15] In the present case, molybdenum coordination with two lattice oxygen atoms of a T_3 Al, as illustrated in the Supporting

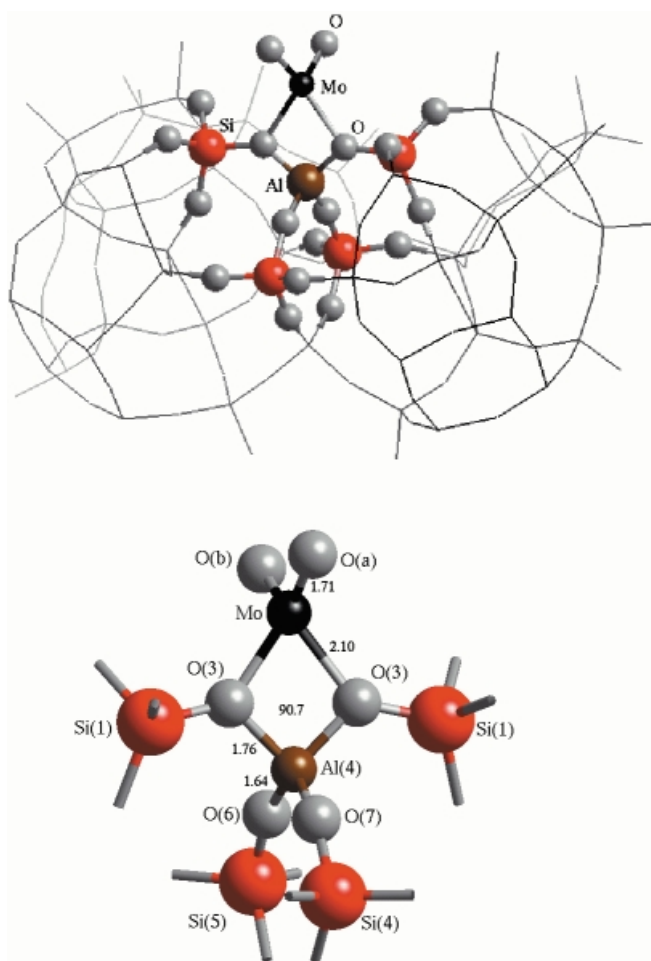


Figure 3. Coordination of molybdenum to the framework of the zeolite.

Information, induce a significant perturbation to the pair of the Al–O bonds and the corresponding O–Al–O bond angle, (the AlO_4 geometry has been lowered from near T_d to C_{2v}), hence resulting in a greater EFG at Al (Figure 3). DFT computation indicates that charge symmetry perturbation resulting from bonded Mo extensively enlarges the EFG at Al,^[18] thus a larger SOQE.^[15b,c, 17] As pointed out by van Santen et al.,^[17] the method used to calculate EFG and, therefore, SOQE etc., aims for reliable geometries and relative trends of the EFG rather than the correct absolute values. Bearing this in mind, the calculated SOQE value of signal F is about 11.3 MHz, which reasonably agrees with the value determined by MQ MAS NMR experiments. We must mention here that the low intensity of signal F hinders the accurate determination of the NMR parameters; this could also account for the difference between the experimental and theoretical SOQE values. Therefore, the effect of site-symmetry lowering at Al makes possible the detection of a distorted tetrahedral aluminum framework species (F) with a large SOQE in the two-dimensional ^{27}Al MQ spectra.

Therefore, we conclude that the larger SOQE of the new species observed in the ultra high-field MAS NMR and two-dimensional MQMAS NMR spectra supports the model of direct metal-bonding to the zeolite framework (Figure 3). If this kind of interaction is strong enough, aluminum will be extracted out of lattice by Mo, forming nonframework $\text{Al}_2(\text{MoO}_4)_3$ (its hydrated form is signal E). In short, we have confirmed the existence of strong interaction between guest and zeolite, that is, a metal center within zeolitic channel which is responsible for the initial transformation of reactant. Whereas A, B, and C correspond to framework Al atoms that are inert to adsorption with Mo, they still bind to protons, retain their Brønsted nature and participate in succeeding catalytic reactions.^[5] Similar results were obtained in the study of Rh/MCM-22 and La/Beta ($\delta_{\text{iso}} \approx 62\text{--}67$ ppm; SOQE $\approx 6.0\text{--}7.0$ MHz).

In summary, this work demonstrates that the presence of metal-distorted tetrahedral aluminum species, resolved in the ultra high-field and high-speed ^{27}Al MAS NMR or two-dimensional ^{27}Al MQ MAS NMR experiments, can be taken as a tangible criteria for the identification of interaction between metals loaded onto zeolite frameworks. These NMR experiments provide a sufficiently general method for the investigation of guest–zeolite interactions.

Experimental Section

MCM-22 (Si/Al = 15) zeolite was synthesized according to Rubin and Chu (U. S. Patent 4 954 325, 1990) by using hexamethyleneimine (HMI) as the directing agent. The crystalline structure (MWW) of the as-synthesized zeolites was confirmed by X-ray diffraction (D/max-rB diffractometer with $\text{Cu}_{K\alpha}$ radiation), with no hybrid crystallites observed. The protonated form of the zeolite was obtained by exchanging the Na^+ three times with NH_4NO_3 solution (1 mol L^{-1}); it was then washed and dried at 373 K, heated to 823 K at 10 K min^{-1} , and kept at 823 K for 4 h. The catalyst 6 wt % Mo/HMCM-22, which has the best catalytic performance in methane dehydroaromatization reaction, was obtained by impregnating HMCM-22 powder (10 g) with an aqueous solution (20 mL) containing the desirable amount of ammonium heptamolybdate (AHM), then dried at RT for 12 h. The samples were further dried at 373 K for 8 h and calcined in air

at 773 K for 3–4 h. Before the NMR experiments, the samples were kept in a desiccator filled with aqueous NH_4Cl solution for more than 120 h to get fully hydrated samples. The 6 wt % Mo/MCM-22 is denoted as Mo/MCM-22 through out this manuscript.

^{27}Al MAS NMR spectra were recorded on a Bruker DRX-833 NMR spectrometer, with an operating frequency for ^{27}Al of 217.62 MHz, equipped with a home-made MAS probe using 2 mm rotor. The measurements were performed by using an excitation pulse length of $2\text{ }\mu\text{s}$ with a spin rate of 19.1–21.1 kHz. 512 scans were used to accumulate the signals with a recycle delay of 5 s. ^{27}Al triple-quantum MAS NMR spectra were recorded on a Bruker ASX-300 NMR spectrometer with an ^{27}Al operating frequency of 78.2 MHz. The 4 mm rotors were spun at 12 kHz. To produce pure-absorption line shapes in the 3Q MAS spectra, a simple two-pulse sequence was used, and the conditions for excitation and transfer of the ($\pm 3Q$) coherence were optimized. The phase cycling was composed of six phases for the selection of the triple-quantum. The phase cycling was combined with a classic overall four-phase cycle in order to minimize phase and amplitude mis-setting of the receiver. A recycling time of 0.5 s was used, as the relaxation for ^{27}Al in solid is generally fast. A $12\text{ }\mu\text{s}$ increment was used for 3Q MAS. The $t_2 \times t_1$ matrix was 512×256 and F_1 dimensions were zero-filled to 512 points before Fourier transformation. In the 3Q experiments, the maximum signals were obtained when the duration of the excitation and detection pulses were 3 and $1\text{ }\mu\text{s}$, respectively. The radio frequency field strength was 143 kHz. 420 transients were taken for each t_1 increment. After measurements of 3Q MAS, the “shearing” was performed by using a home-built custom program. The chemical shift was referenced to $[\text{Al}(\text{H}_2\text{O})_6]^{3+}$.

The isotropic chemical shift as well as the parameter for second-order quadrupolar effect (SOQE) is estimated from the spectrum by using the Equations (1) and (2):

$$\delta_{\text{iso}}(i) = 4/3 \delta_1(i) - 1/3 \delta_2(i) \quad (1)$$

$$\text{SOQE}(i)^2 = C_q(i)^2(1 + \eta(i)^2/3) = (\delta_{\text{iso}}(i) - \delta_2(i))\nu_0^2/6000 \quad (2)$$

In Equations (1) and (2) $\delta_{\text{iso}}(i)$ is the isotropic chemical shift and $\delta_1(i)$ and $\delta_2(i)$ are the coordinates of the center of gravity of signal (i) in the F_1 and F_2 dimensions, respectively. $C_q(i)$ is the quadrupolar coupling constant, $\eta(i)$ is the asymmetry parameter and ν_0 is the larmor frequency of the ^{27}Al nucleus. The results are summarized in Table 1.

Using the Monte Carlo calculation method and density functional theory,^[18] we studied the molybdenum species of Mo/HZSM-5 catalyst. In this model, Mo was coordinated to two oxygen atoms of the zeolites, therefore two Mo–O–Al bonds were formed. For the MCM-22-supported molybdenum catalysts, although the location of such a cluster probably varies, the nature of the active centers may remain the same.

The set up of the Mo-bound AlO_4 model was similar to that reported previously.^[18] We defined a penta-tetrahedral cluster (T5) around the molybdenum atom, and the structure refinement was completed by using density functional theory (DFT). The optimization detail was similar to that reported previously. The molybdenum was located in tetrahedral aluminum framework at the T_3 site of $P6mm$ model (see Figure 3).^[8] To obtain a rational model of the active Mo center, we performed a two-step calculation. First the model of the zeolite cluster with the Si–O–Al bridge was optimized. Next the Mo species bonding to ZSM-5 cluster was constructed and optimized. The dangling silicon and oxygen bonds were terminated with hydrogen atoms, whose positions were optimized by molecular mechanics minimization. All results presented in this work were obtained by means of DFT. The calculations were carried out by using the DMol 3 software in Cerius 2 (version 4.2; Molecular Simulations Inc.). The calculations were run on the SGI O2 workstation. Optimization was done within the local density approximation (LDA) by using the Janak–Moruzzi–Williams (JMW) functional. The basis set was selected as doubly numerical with polarization (DNP). The atomic core representation of ECP (relativistic effective core potentials) was selected in which all-electron calculations were done for H, O, Si and Al atoms, whereas the Mo atom was presented by a (4s,4p,4d,5s) valence basis sets with the $[\text{Ar}]3d^{10}$ core described by a model core potential. The model was optimized by using spin-restricted procedures. We set the self-consistent-field parameters so that the total energy converged to 1×10^{-5} hartree.

According to reference [17], the calculation of C_q and the asymmetry parameter of the EFG is achieved through Equations (3)–(5):

$$C_q = -34.9647 V_{zz} Q \quad (3)$$

$$\eta = \frac{|V_{xx} - V_{yy}|}{V_{zz}} \quad (4)$$

$$V(r) = \sum_A \frac{Z_A}{|r - R_A|} - \sum_{\mu\nu} P_{\mu\nu} \int \frac{\phi_\mu(r_1) \phi_\nu(r_1)}{|r - r_1|} dr \quad (5)$$

Acknowledgement

Financial support from the National Natural Science Foundation of China and the Ministry of Science and Technology of China, Project No. G1999022400, are gratefully acknowledged.

- [1] A. Corma, *Chem. Rev.* **1995**, 95, 559.
- [2] G. C. Bond, *Catalysis by Metals*, Academic Press, New York, **1962**.
- [3] a) P. Meriaudeau, C. Naccache, *Catal. Rev.-Sci. Eng.* **1997**, 39, 5; b) B. S. Kwak, W. M. H. Sachtler, *J. Catal.* **1994**, 145, 456; c) M. Hartmann, L. Kevan, *Chem. Rev.* **1999**, 99, 635.
- [4] a) J. L. G. Fierro, J. C. Conesa, A. L. Agudo, *J. Catal.* **1987**, 108, 334; S. Huang, C. Shang, C. Yuan, Y. Li, Q. Wang, *Zeolites* **1990**, 10, 772; b) V. R. Choudhary, A. K. Kinage, T. V. Choudhary, *Science* **1997**, 275, 1286; J. Yao, R. Le van Mao, M. S. Kharson, L. Dufresne, *Appl. Catal.* **1992**, 65, 670; c) G. L. Price, V. Kannzirev, D. F. Church, *J. Phys. Chem.* **1995**, 99, 864; L. Rodriguez-Santiago, M. Sierka, V. Branchadell, M. Sodupe, J. Sauer, *J. Am. Chem. Soc.* **1998**, 120, 1545; d) M. Hartmann, L. Kevan, *J. Phys. Chem.* **1996**, 100, 4606; e) K. Okumura, M. Niwa, *J. Phys. Chem.* **2000**, 104, 9679; L. J. Lobree, I. Hwang, J. A. Reimer, A. T. Bell, *J. Catal.* **1999**, 186, 242; M. Shelef, *Chem. Rev.* **1995**, 95, 209; f) G. D. Pirngruber, K. Seshan, J. A. Lercher, *J. Catal.* **2000**, 190, 396; g) D. Ma, Y. Shu, M. Cheng, Y. Xu, X. Bao, *J. Catal.* **2000**, 194, 105.
- [5] D. Ma, Y. Shu, W. Zhang, W. Han, Y. Xu, X. Bao, *Angew. Chem.* **2000**, 112, 3050; *Angew. Chem. Int. Ed.* **2000**, 39, 2928.
- [6] M. J. Rice, A. K. Chakraborty, A. T. Bell, *J. Catal.* **2000**, 194, 278.
- [7] a) H. G. Karge, B. Wichterlova, H. K. Beyer, *J. Chem. Soc. Faraday Trans.* **1992**, 88, 1345; b) A. V. Kucherov, A. A. Slinkin, *Zeolites* **1987**, 7, 583; c) D. Ma, W. Zhang, Y. Shu, X. Liu, Y. Xu, X. Bao, *Catal. Lett.* **2000**, 66, 155.
- [8] M. K. Rubin, P. Chu, U.S. Patent, 4954325, **1990**.
- [9] S. Unverricht, M. Hunger, S. Ernst, H. G. Karge, J. Weitkamp, *Stud. Surf. Sci. Catal.* **1994**, 84, 37; S. L. Lawton, A. S. Fung, G. J. Kennedy, L. B. Alemany, C. D. Chang, G. H. Hatzikos, D. N. Lissy, M. K. Rubin, H. C. Timken, S. Steuernagel, D. E. Woessner, *J. Phys. Chem.* **1996**, 100, 3788; D. Ma, F. Deng, R. Fu, X. Han, X. Bao, *J. Phys. Chem.* **2001**, 105, 1770.
- [10] a) J. C. Edwards, E. C. Decanio, *Catal. Lett.* **1993**, 19, 121; b) X. Carrier, J. F. Lambert, M. Che, *J. Am. Chem. Soc.* **1997**, 119, 10137; c) W. Kolodziejewski, E. Lalik, A. Lerf, J. Klinowski, *Chem. Phys. Lett.* **1992**, 194, 429; d) D. Wilmar, O. Clause, J.-B. Caillerie, *J. Phys. Chem. B* **1998**, 102, 7023; e) In ref. [10a], the author observed that the model $[\text{Al}(\text{OH})_n(\text{H}_2\text{O})_{6-n}]_n(\text{MoO}_4)$ gives rise to a peak centered at $\delta = 13$ ppm in ^{27}Al MAS NMR spectrum, while it can transform into $(\text{Al}_2(\text{MoO}_4)_3)$ after calcination of the model compound at 773 K.
- [11] J. Rocha, S. E. Carr, J. Klinowski, *Chem. Phys. Lett.* **1991**, 187, 401.
- [12] a) L. Frydman, J. S. Harwood, *J. Am. Chem. Soc.* **1995**, 117, 5367; b) A. Medek, J. S. Harwood, L. Frydman, *J. Am. Chem. Soc.* **1995**, 117, 12779; c) C. Fernandez, J. P. Amoureux, *Chem. Phys. Lett.* **1995**, 242, 449; d) S. E. Lattur, J. Sachleben, B. B. Iversen, J. Hanson, G. D. Stucky, *J. Phys. Chem.* **1999**, 1, 7135; e) C. A. Fyfe, J. L. Bretherton, L. Y. Lam, *Chem. Commun.* **2000**, 1575; f) T.-H. Chen, B. H. Wouters, P. J. Grobet, *Eur. J. Inorg. Chem.* **2000**, 281; g) A. P. M. Kentgens, D. Iuga, M. Kalwei, H. Koller, *J. Am. Chem. Soc.* **2001**, 123, 2925; h) J. C. C. Chan, *Concepts Magn. Reson.* **1999**, 11, 363.
- [13] J. A. van Bokhoven, A. L. Roest, D. C. Koningsberger, J. T. Miller, G. H. Nachttegaal, A. P. M. Kentgens, *J. Phys. Chem. B* **2000**, 104, 6743.
- [14] For the Mo/MCM-22 sample, the dealumination happened after 773 K calcinations; this results in the formation in the nonframework $[\text{Al}(\text{OH})_n(\text{H}_2\text{O})_{6-n}]_n(\text{MoO}_4)$ species at $\delta = 14$ ppm. However, this kind of dealumination also comes from molybdenum-induced dealumination, and without loading of molybdenum, such signal can not be observed (Figures 1 and 2). At the same time, it is reasonable to conclude that the molybdenum-associated aluminum framework species (tetrahedral, signal F in Figure 2) is the precursor of the hydrated aluminum molybdate ($\delta = 14$ ppm). With a more rigorous treatment (higher calcinations temperature, longer calcinations time), more molybdenum-associated framework Al site were transformed into nonframework aluminum molybdate.
- [15] a) P. J. Dirken, G. H. Nachttegaal, A. P. M. Kengens, *Solid State Nucl. Magn. Reson.* **1995**, 5, 189; b) M. Kovalokova, P. J. Grobet, *Solid State Nucl. Magn. Reson.* **1997**, 9, 107; c) G. Engelhardt, W. Veeman, *J. Chem. Soc. Chem. Commun.* **1993**, 622.
- [16] a) D. Freude, J. Klinowski, H. Hamdan, *Chem. Phys. Lett.* **1988**, 149, 35; H. Ernst, D. Freude, I. Wolf, *Chem. Phys. Lett.* **1993**, 212, 588; b) F. Haase, J. Sauer, *J. Am. Chem. Soc.* **1995**, 117, 3780; M. Krossner, J. Sauer, *J. Phys. Chem.* **1996**, 100, 6199.
- [17] H. Koller, E. L. Meijer, R. A. van Santen, *Solid State. Nucl. Mag. Reson.* **1997**, 9, 165.
- [18] D. Zhou, D. Ma, X. Liu, X. Bao, *J. Chem. Phys.* **2001**, 114, 9125.

Received: June 7, 2002 [F4164]